

Article

Robotic Nd:YAG Fiber Laser Welding of Ti-6Al-4V Alloy

Ceyhun Köse ^{1,*} and Engin Karaca ²

¹ Faculty of Natural Sciences and Engineering, Department of Mechanical Engineering, Gaziosmanpaşa University, Tokat 60150, Turkey

² Graduate School of Natural and Applied Sciences, Department of Mechatronics Engineering, Gaziosmanpaşa University, Tokat 60150, Turkey; engin.karaca@gop.edu.tr

* Correspondence: ceyhun.kose@gop.edu.tr; Tel.: +90-356-252-1800; Fax: +90-356-252-1729

Received: 10 April 2017; Accepted: 13 June 2017; Published: 15 June 2017

Abstract: In the present study, Ti6Al4V titanium alloy plates were joined using a robotic fiber laser welding method. The laser welding process was carried out at two different welding speeds. Effects of different heat input conditions on the microstructure and mechanical properties of robotic fiber laser welded joints were investigated. Some grain coarsening was observed in the microstructure of weld metal in samples joined using high heat input, compared to those using low heat input, and volume rates of primary α structures increased in the weld metal. The microstructure of weld metal in samples joined using low heat input was made of basket-weave or acicular α' grains and primary β grains in grain boundaries. Tensile and yield strength of samples joined using low heat input were higher than for those joined using high heat input, but their ductility was lower.

Keywords: titanium alloy; fiber laser welding; microstructure; mechanical properties

1. Introduction

Ti6Al4V is the most used and preferred titanium alloy. Ti6Al4V is an $\alpha + \beta$ group alloy in which aluminum is the α stabilizer and vanadium is the β stabilizer [1,2]. Due to its low density, heat resistance, high mechanical strength, corrosion resistance, and biocompatibility properties, the Ti6Al4V alloy has a wide range of uses [3,4]. The Ti6Al4V alloy is used in jet engines, spacecraft, missiles, the auto industry, pressure vessels, orthodontics, medical implants and surgical tools [5]. TIG (Tungsten Inert Gas), friction welding, friction stir welding, plasma arc, electron beam and laser beam welding methods can be used for welding the Ti6Al4V alloy [3]. When welded joints of titanium alloys are conducted using high heat input, a high level of distortion and contamination risk are involved. Temperatures of over 500 °C in welded joints of Ti6Al4V lead to absorption of deleterious gases such as oxygen, nitrogen and hydrogen in the welding seam, leading to lower mechanical strength [6]. Slower cooling due to high heat input in the welding of titanium and its alloys results in grain coarsening and porosity formation in the welding seam [7]. Grain coarsening and porosities cause lower mechanical strength, especially in welded joints. In welding titanium and its alloys, a narrow welding seam and a microstructure made of fine grains should be achieved by lowering the heat input transfer to the weld zone, and increasing the cooling rate. On the other hand, very fast cooling conditions lead to weld metal microstructures that are completely martensitic in nature, and thus have a lower toughness [8].

Laser welding differs from traditional welding methods on account of its lower heat input, higher condensation energy, faster welding speed, narrower weld zone, its ability to produce joints with deeper penetration, its higher mechanical strength, lower distortion, and its ability to weld without the use of additional metal [9–16]. Fiber laser welding machines have been used for decades. They work at between 100 W average power and 6 kW peak power. The most important advantage of fiber lasers

is the easiness of laser control, due to the wave length of the laser beam. Energy is easily transferred through fiber optical cables. The fiber laser welding method, on the other hand, has advantages of lower beam distortion rate, flexible beam distribution, lower maintenance cost, higher efficiency and high quality welded joints [17]. In contrast to traditional welding methods, laser welding provides control over heat input, making it possible to achieve the desired metallurgical properties and mechanical strength levels in welded joints of the Ti6Al4V alloy. In the present study, Ti6Al4V plates were joined using a robotic Nd:YAG (neodymium-doped yttrium aluminum garnet) fiber laser. The effects of welding speed on the microstructure and mechanical properties of laser welded Ti6Al4V alloy were investigated.

2. Experimental Studies

2.1. Material and Welding Process

In the present study, Ti6Al4V alloy, an alloy preferred in many areas of industry, was used. Its chemical composition is given in Table 1.

Table 1. The chemical composition of Ti6Al4V (wt %).

C%	Al	V	Fe	N	O	H	Ti
0.010	6.02	4.14	0.098	0.007	0.12	0.0020	Balance

Experimental material was prepared with dimensions of 100 mm × 330 mm × 4 mm for the welding process. Experimental samples were joined in a flat position using a FANUC ROBOT R-2000 iB 210F Nd:YAG fiber laser welding machine with 4 kW power (Fanuc, Yamanashi Prefecture, Japan), without using any additional metal (Figure 1). The welding parameters are given in Table 2.



Figure 1. The laser welding process and fixing clamps.

Table 2. The laser welding parameters.

Sample	Laser Power (W)	Travel Speed (mm/s)	Shielding Gas	Gas Pressure (bar)	Focal Length (mm)	Heat Input (kJ/mm)
A1	1500	6	He	1	190	0.25
A2	1500	9	He	1	190	0.16

2.2. Mechanical Tests and Characterization of Microstructure

In order to determine mechanical properties of welded joints, four test samples were prepared for each parameter, based on the ISO 4136:2012 standard for the tensile test, and on the ISO

9016:2012 standard for the impact notch test. The tensile test was conducted using an INSTRON tensile test machine with 100 kN capacity (Instron, MA, USA) at a 10 mm/min crosshead speed. The impact notch test, on the other hand, was carried out at room temperature using an ALŞA testing machine (Alşa, Istanbul, Turkey). Hardness measurement was performed by a GALILEO test machine (GALILEO, Antegnate, Italy) applying 200 g to the tip for 15 s. For determination of microstructural changes, an etching procedure using Kroll's solution was used. A NIKON optic microscope (5–100 \times magnification, Nikon, Tokio, Japan) JEOL JSM 6060 LV and JEOL JSM 7001 LV scanning electron microscope (SEM, Jeol Ltd., Tokyo, Japan) and OXFORD X-MAX 80 (energy dispersive spectrometer, EDS) equipment (Oxford Instruments, Oxfordshire, UK) were used for microstructural examinations.

3. Results and Discussion

3.1. Macro and Microstructural Examinations

Macro images belonging to A1 and A2 samples are shown in the Figure 2. As can be understood from the macro images, undercut, underfill and cracks were not observed in the welding seam, but cracks were observed in optical microscope image (Figure 5b).



Figure 2. Macro images of laser welded joints, (a) A1 Sample, (b) A2 Sample.

It was observed that the microstructure of the base metal was made of equiaxed α grains (light colored grain, hexagonal close packed) and β grains in grain boundaries (dark colored grain, body centered cubic) (Figure 3).



Figure 3. Microstructure image of base metal.

Equiaxed grain structures in the base metal increase fracture toughness and support strength [18]. The HAZ (Heat Affected Zone) and weld metal microstructure depend on no filler metal being used with the melting of base metal. It is known that when additional filler metal is used, major differences arise in the HAZ and the weld metal microstructure. Microstructure shapes with respect to the chemical composition of alloy and cooling rate. Fine grained microstructure forms in the weld metal. However, grain coarsening can be expected with use of high laser power, or with joints carried out at very slow welding speeds. During the solidification process, β grains display growth in the direction of the heat flow [19].

Due to the occurrence of a rapid cooling regime, a dominant martensitic microstructure exists in the weld metal of Ti6Al4V alloy joined by laser welding. In addition, with an increase of heat input, transformed beta grains with acicular alpha grains can form in the weld metal. In the HAZ and weld metal microstructure images for the study (Figure 4), a dominant martensite microstructure, cellular dendrite and columnar dendrite occurred, due to the rapid cooling related to the low heat input that is a characteristic feature of the laser welding method.

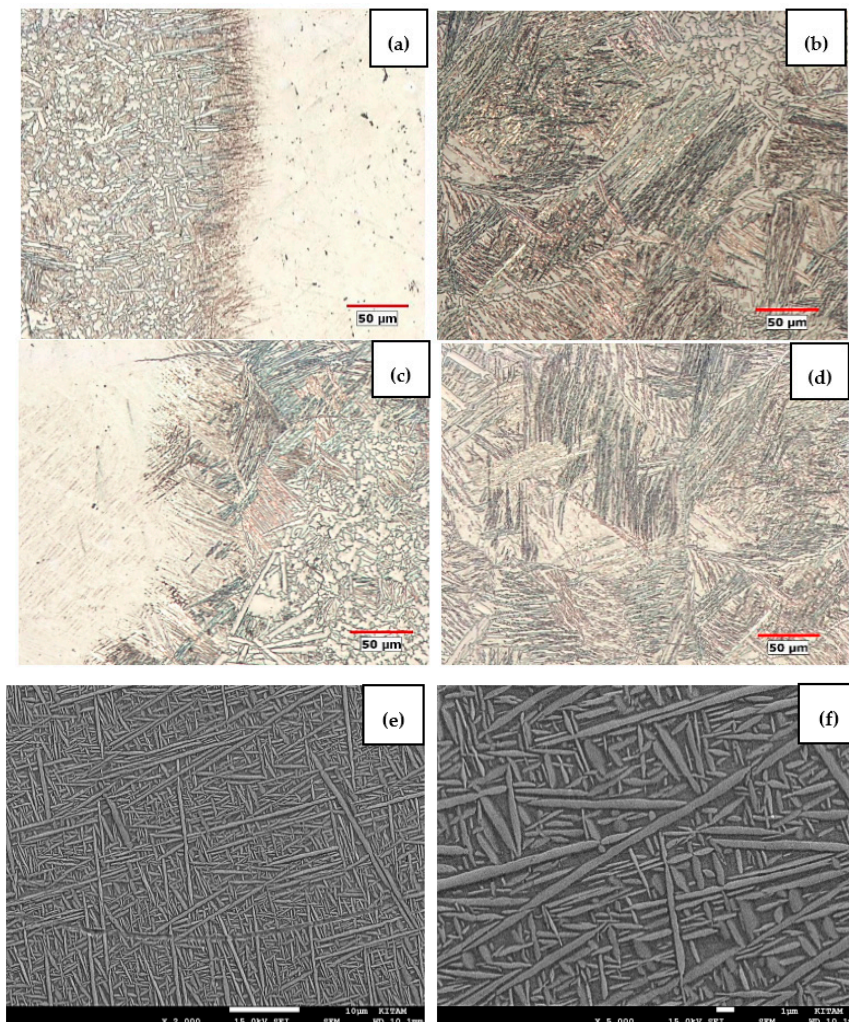


Figure 4. Microstructure images of the welded joint, (a) heat affected zone (HAZ); and (b) weld metal of A1 sample; (c) HAZ; and (d–f) weld metal of A2.

When the microstructures of the welded joints were investigated, it was observed that the HAZ arises from fine acicular α' martensite and primary α structures due to fast cooling (Figure 4). These types of microstructures can be observed at cooling temperatures lower than the β transus

temperature [20]. It has been reported that cooling rates higher than 410 °C/s should be achieved to obtain a fully martensitic microstructure in Ti6Al4V alloy [3,21]. Studies reported that when the base metal is heated to temperatures over the β transus temperature during welding, martensite phase transformation from the high-temperature β phase takes place, and α' is formed with the basket weave [22]. At cooling rates slower than 410 °C/s, on the other hand, transformed α phase occurs preferentially in the primary β grain boundary. Figure 4 shows that cooling rate as a function of laser welding parameters, i.e., as a function of heat input, affected HAZ width. Because of joining using low heat input, a narrow HAZ developed. Some grain coarsening occurred due to the weld thermal cycle in the HAZ microstructure of samples joined using high heat input. It was observed that the weld metal microstructures of samples especially joined using low heat input was composed of basket-weave, acicular α' grains and primary β grains in the grain boundaries. As a result of the slower cooling rate in laser welding due to the low heat input, a diffusionless transformation of β phase into a martensitic structure takes place. In addition, local microcrack formation was observed in the weld metal of samples joined using low heat input (Figure 5b). Crack formation is always possible in welded joints like laser welding, where cooling is fast [5]. Presence of martensite, a hard and brittle phase, is among the major factors triggering the formation of microcracks in welded joints of titanium alloys and stainless steels. There may always be crack risk in the welding seam under rapid cooling conditions. Especially in laser beam welding, the occurrence of a rapid solidification rate can increase crack risk. To be able to decrease crack risk, it is suggested that samples should be fixed on the ground using clamps during welding [5]. In this study, samples were fixed on the ground using clamps during welding (Figure 1). Titanium alloys are reactive with ambient gases at high temperatures. For this reason, a shielding gas was used to protect the molten weld pool against oxidation until enough cooling had occurred. In spite of these protective conditions, crack and porosity formation were observed in the weld metal of the A2 sample. The crack occurrence in the A2 sample indicates that the molten weld pool was not protected as expected during the welding process. Setting the gas pressure incorrectly could conceivably be the cause of this result. As is well known, titanium alloys are quite resistant to crack risk. Weld cracking, however, can still be caused by contamination cracking, such as hydrogen-delayed cracking or liquation of iron-rich eutectic [3]. In this study, it should also be stated that cracks occurred in the weld metal of the A2 sample carried out locally. Less coarsened columnar β grain structures were observed in weld metal than in the HAZ (Figure 4). The volume rate of primary α structures increased in the weld metal of samples joined using high heat input. Besides, porosity formations were observed in weld metal microstructures (Figure 5a). Porosity formation is frequently encountered in laser welded titanium alloys. Gas type porosities arise especially from hydrogen, which cannot be removed from the weld pool during the solidification of the welding seam [23]. Porosity formation is expected to lower the mechanical strength of welded joints.

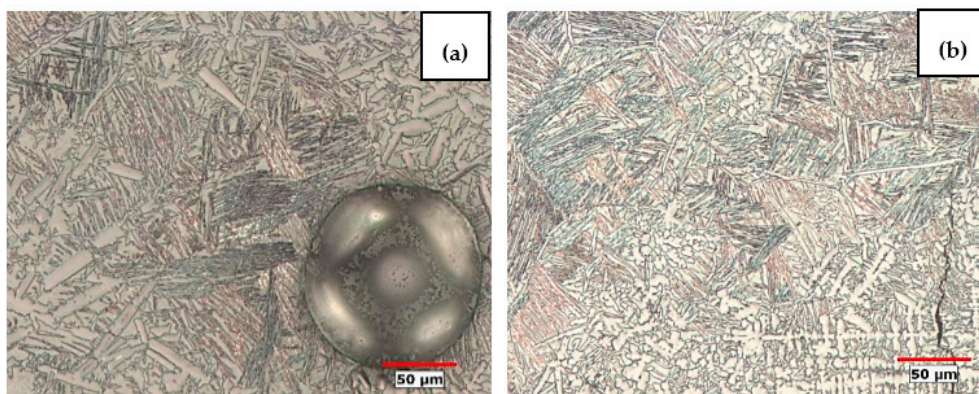


Figure 5. Porosity formation (a) with local crack formation; and (b) in the weld metal of A2 sample.

EDS analysis performed on welded samples showed that no major element losses occurred in the base metal, HAZ or weld metal (Figure 6). Based on these findings, it can be stated that heat input did not have any negative effect on laser welded joints.

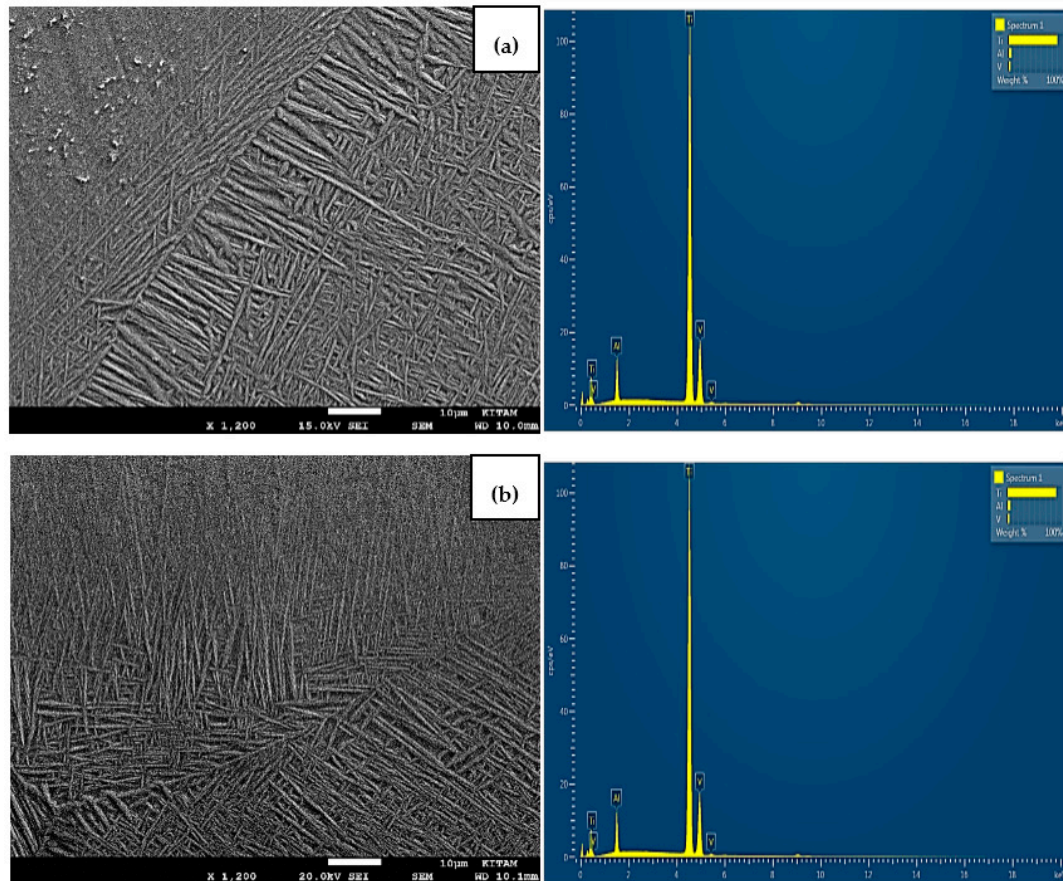


Figure 6. Energy dispersive spectrometer (EDS) analysis of base metal, HAZ and weld metal, respectively. (a) A1 Sample, (b) A2 Sample.

3.2. Tensile Test

Tensile testing was carried out to determine the mechanical properties of the base metal (A sample) and laser welded A1 and A2 samples. Results are given in Table 3.

Table 3. The tensile test results of base metal and laser welded samples.

Sample	Tensile Strength (MPa)	Yield Strength (MPa)	Elongation (%)	Fracture Location
A	1057	965	18.5	-
A1	830	720	8.5	HAZ
A2	840	724	8	Weld metal

Results of the tensile experiment revealed that tensile strength, yield strength and percentage elongation of the base metal were higher than those of laser welded samples joined using different heat inputs. Porosities, microcracks and microstructural transformations occurring in the welding seam are among the possible reasons for lower mechanical strength of welded joints compared to the base metal. The sample joined using low heat input (A2 sample) had higher tensile and yield strength, but a lower percentage elongation compared to the sample joined using high heat input (A1 sample). The laser welded A2 sample had a tensile strength of 840 MPa and a ductility level

of 8%, while the laser welded A1 sample had a tensile strength of 830 MPa and a ductility level of 8.5%. As a result of the increase in heat input transferred to the weld zone, coarsening in grain sizes caused a decrease in tensile and yield strength, even in small amounts. Lower ductility in welded $\alpha + \beta$ alloys depends on coarsened primary β grain ratio and the formation of intragranular acicular microstructures [24]. Microsegregations occurring during the solidification of welding seam are also among the factors lowering ductility. After tensile testing, fractures occurred in the weld metal of the A2 sample, while fractures in the A1 sample occurred in the HAZ. It could be expected that fractures in A2 sample would be in the HAZ and fracture in the A1 sample would be in the weld metal; but, as a result of microstructural transformations occurring in the HAZ or weld metal (mostly because of grain coarsening), the cause for these results can be thought to be localized or heterogeneous plastic strains occurring in the welded joints during tensile testing.

When SEM images of fracture surfaces of the base metal and the laser welded samples were examined after tensile testing (Figure 7), it could clearly be seen that ductile fracture, which is a typical fracture mode for titanium, was observable in the base metal and A2 samples by looking at dimples. In addition, for the A1 sample, intragranular fracture occurred with a tear ridges fracture mode. Because welded joints have lower ductility than the base metal after tensile testing, base metal experienced the ductile dimple fracture mode. There were little signs of plastic deformation in the welded A1 sample, with the fracture path appearing to be intergranular along colony boundaries, or cleavage across colonies, which indicates that the fracture mode changed from ductile to cleavage fracture mode [25]. In addition, it is thought that microstructural transformations and loading rates play a significant role in fracture mode changes. The fracture surface morphology of the welds was much rougher than that of the base metal. There were lots of dimples with different sizes and depths in the fracture surfaces of the joints in A1, and obvious tear ridges as well. No inclusion formation was observed in the fracture surface images of welded joints.

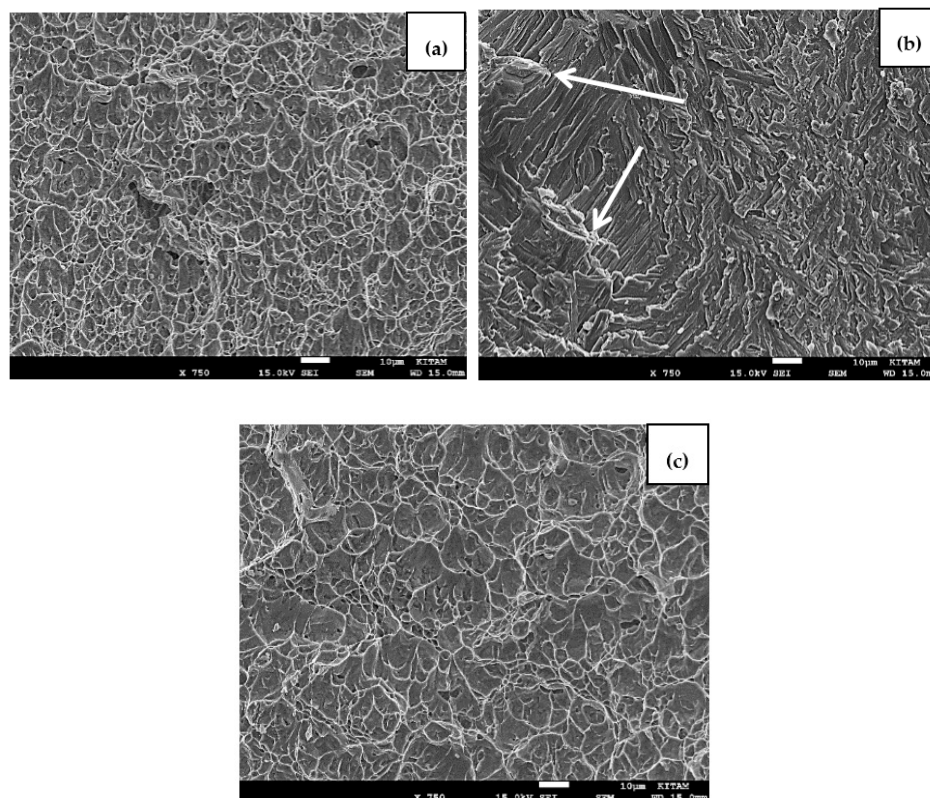


Figure 7. Fracture surface images of base metal and laser welded samples after the tensile test. (a) Base metal, (b) A1 Sample, and (c) A2 Sample, tear ridges indicated by arrows.

3.3. Charpy V-Notch Impact Test

The impact toughness of the base metal and the laser welded samples was determined at room temperature. The impact toughness of the base metal was higher than that of the laser welded samples (17, 13 and 14 J, respectively). The impact toughness of the sample joined using slow welding speed i.e., higher heat input, was higher than that of the sample joined using low heat input (14 and 13 J, respectively). Other investigators who obtained similar findings also stressed that, in order to increase the impact toughness of titanium alloys, martensite structures should be transformed into acicular α or Widmanstätten α grain structures by increasing the heat input, which occurs as a result of using either a lower welding speed or a higher laser power [26]. Cooling rate has an extremely important effect on the mechanical properties of $\alpha + \beta$ alloys. It was stressed that toughness decreases are experienced at fast cooling conditions, due to the formation of finer structured α platelets, while at slower cooling rates, toughness is improved by diverting crack propagation paths with the coarsening of α platelets [27].

Fracture surfaces of the base metal and welded samples after impact testing were examined using SEM (Figure 8). The base metal was broken in ductile fracture mode, while A1 and A2 samples had fractures in the mode of intergranular fractures with either a quasi-cleavage type or tear ridges.

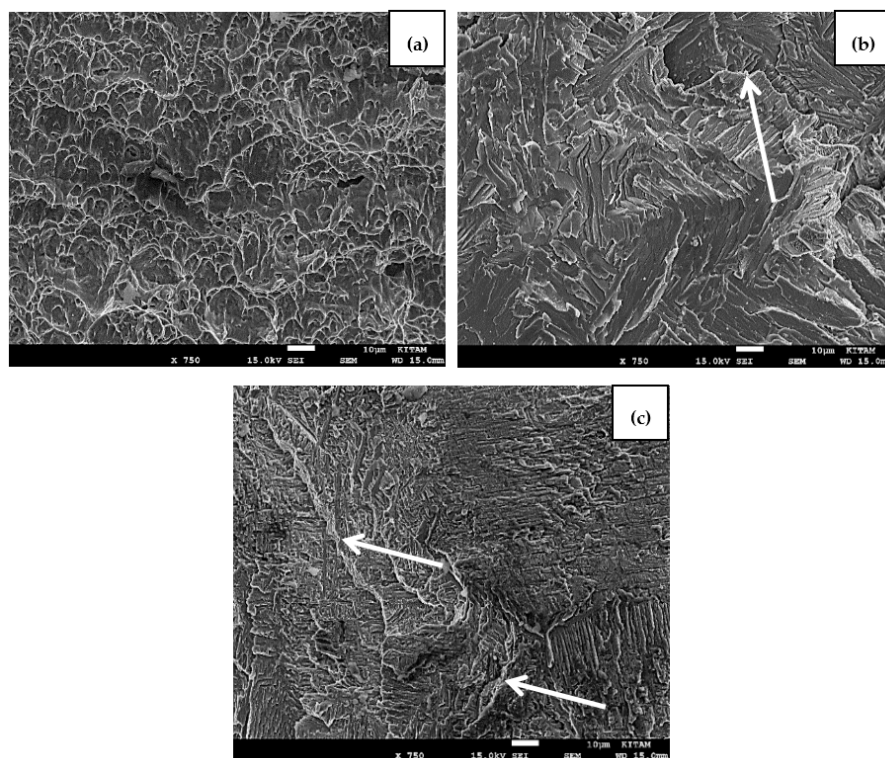


Figure 8. Fracture surface images of base metal and laser welded samples after The Charpy V-notch impact test. (a) Base metal, (b) A1 Sample, (c) A2 Sample, tear ridges indicated by arrows.

3.4. Microhardness

Due to the higher power intensity of laser welding, when compared to traditional welding methods, it results in low heat input and fast solidification, leading to high hardness levels in the welded joints. Distributions of hardness in welded joints is directly related to microstructure, and martensite in the microstructure is the most important factor for the hardness increase in the HAZ and weld metal of Ti6Al4V alloy. When the average hardness levels of samples joined using different welding speeds—i.e., different heat input, were examined, it was found that the hardness of the weld metal and HAZ was higher than for the base metal (Figure 9).

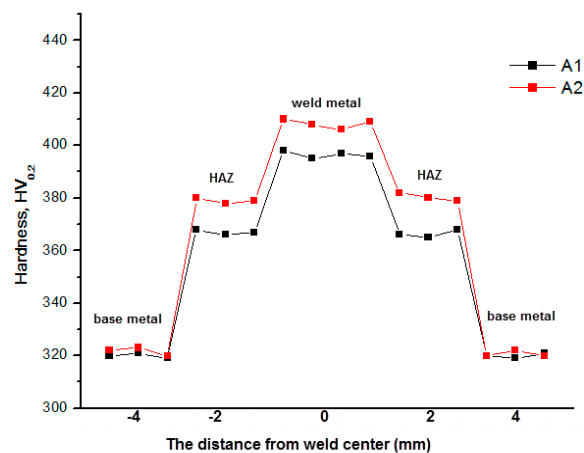


Figure 9. Microhardness distributions in the welded joints.

The reason for this outcome has been reported to be the formation of harder and finer acicular α' martensite structures in the weld metal and HAZ, compared to the structure of the $\alpha + \beta$ base metal [28,29]. Hardness level was observed to decrease as either laser power increased or welding speed decreased; i.e., as heat input increased. Investigators reported that hardness levels decreased as a result of coarsened primary β structure due to higher heat input [29]. With lower heat input, on the other hand, an increase in hardness is expected, owing to the formation of finer-grained α' structures [23]. The reason for the increase of hardness in weld metal compared to base metal was reported to be compact regions of α' with high-density dislocations and phase boundaries [22]. Hardness of the weld metal was determined to be higher than that of the HAZ for both welding speeds. It has been explained by some investigators that the decrease in hardness from weld metal to HAZ was caused by the decreased martensite content and Widmanstätten α structure [30]. When hardness results were examined generally, hardness levels of the HAZ and weld metal were similar. This similarity was linked to the very low heat conduction coefficient ($6.7 \text{ W} \cdot \text{m}^{-1} \cdot \text{K}^{-1}$) of Ti6Al4V alloy [31]. Thermal energy transferred to the weld zone of Ti6Al4V alloy can stay there longer before dispersing [31]. The higher hardness in the HAZ and weld metal compared to the base metal is expected to produce more strength in the joints than in the base metal. A similarity was expected between the hardness and tensile strength results. Nevertheless, such a similarity was not observed in the present study, due to the presence of porosities and microcrack formations in the weld metal and HAZ.

4. Conclusions

(1) The microstructure of the base metal comprised equiaxed α grains, while the weld metal structure displayed a martensitic microstructure formation because of fast cooling at both welding speeds. Slight grain coarsening was observed in the HAZ and weld metal of the sample joined using high heat input. Some porosity and local microcrack formations were observed in the weld metal microstructure. The crack occurrence in the A2 sample indicates that the molten weld pool was not protected as expected during welding process. Setting the gas pressure incorrectly may be a potential cause of this result. As is well known, titanium alloys are quite resistant to crack risk. The weld cracking, however, can still be caused by contamination cracking, such as hydrogen-delayed cracking or liquation of iron-rich eutectic.

(2) Based on tensile testing, the strength of the base metal was higher than that of the laser welded joints. Such an outcome could be due to porosity formations observed in the welding seam, as well as to possible microcracks that might have occurred in the welding seam. The tensile and yield strength of samples joined using low heat input were higher than those of samples joined using high heat input, but percentage elongation was higher in samples joined using high heat input. After tensile testing,

fracturing in the A2 sample occurred in the weld metal, while fracturing in the A1 sample occurred in the HAZ. As a result of microstructural transformations occurring in the HAZ or weld metal (mostly because of grain coarsening), it is thought that localized or heterogeneous plastic strain occurring in welded joints during tensile testing may have caused these results. While fractures after tensile testing occurred in the form of ductile fractures for the base metal and A2 samples, the A1 samples exhibited intragranular fractures occurring with a tear ridges fracture mode. Because the twelded joints show less ductility than the base metal after tensile testing, the base metal exhibited a ductile dimple fracture mode. There were minor signs of plastic deformation in the welded A1 sample, with the fracture path appearing to be either intergranular along colony boundaries or cleavage across colonies, which indicates that the fracture mode changed from a ductile to a cleavage fracture mode.

(3) Impact toughness was lower in laser welded joints than in the base metal. Impact toughness of the material joined using lower welding speed i.e., with higher heat input, was higher than that of samples joined using low heat input. Among the leading causes increasing impact toughness with higher heat input is the transformation of martensite structures to acicular α or Widmanstätten α grain structures. After impact testing, the base metal was broken in a ductile fracture mode, while the A1 and A2 samples had fractures in the mode of intergranular fracture with a quasi-cleavage type.

(4) In terms of the hardness of samples joined using different heat inputs, the hardness of the weld metal and HAZ was higher than that of the base metal. The hardest zone was the weld metal. Increasing laser power or decreasing welding speed i.e., increasing heat input, both resulted in lower hardness. Coarsening of primary β structures, which is a result of increased heat input, led to lower hardness.

Acknowledgments: The authors thank Zafer TATLI and research assistants at Sakarya University, Faculty of Technology, Metallurgical and Materials Engineering Department; Uğur KÖLEMEN, Fikret YILMAZ and the research assistants at Gaziosmanpaşa University, Faculty of Applied Sciences; and KİTAM of Samsun 19 Mayıs University for their valuable contributions.

Author Contributions: Ceyhun Köse and Engin Karaca conceived and designed the experiments; Ceyhun Köse and Engin Karaca performed the experiments and analyzed the data; Ceyhun Köse wrote the paper.

Conflicts of Interest: The authors declare no conflict of interest.

References

1. Donachie, M.J. *Titanium: A Technical Guide*; ASM International: Geauga County, OH, USA, 2000.
2. Leyens, C.; Peters, M. *Titanium and Titanium Alloys*; WILEY-VCH Verlag GmbH & Co. KGaA: Weinheim, Germany, 2003.
3. Cao, X.; Jahazi, M. Effect of welding speed on butt joint quality of Ti-6Al-4V alloy welded using a high-power Nd:YAG laser. *Opt. Lasers Eng.* **2009**, *47*, 1231–1241. [[CrossRef](#)]
4. Yıldız, A.; Kaya, Y.; Kahraman, N. Joint properties and microstructure of diffusion-bonded grade 2 titanium to AISI 430 ferritic stainless steel using pure Ni interlayer. *Int. J. Adv. Manuf. Technol.* **2016**, *86*, 1287–1298. [[CrossRef](#)]
5. Akman, E.; Demir, A.; Canel, T.; Sınmazçelik, T. Laser welding of Ti6Al4V titanium alloys. *J. Mater. Process. Technol.* **2009**, *209*, 3705–3713. [[CrossRef](#)]
6. Gao, X.L.; Zhang, L.J.; Jing, L.; Zhang, J.X. A comparative study of pulsed Nd:YAG laser welding and TIG welding of thin Ti6Al4V titanium alloy plate. *Mater. Sci. Eng. A* **2013**, *559*, 14–21. [[CrossRef](#)]
7. Balasubramanian, T.S.; Balakrishnan, M.; Balasubramanian, V.; Manickam, M.M. Influence of welding processes on microstructure, tensile and impact properties of Ti-6Al-4V alloy joints. *Trans. Nonferr. Met. Soc. China* **2011**, *6*, 1253–1262. [[CrossRef](#)]
8. Murthy, K.K.; Sundaresan, S. Phase transformations in a welded near- α titanium alloy as a function of weld cooling rate and post-weld heat treatment conditions. *J. Mater. Sci.* **1998**, *33*, 817–826. [[CrossRef](#)]
9. Köse, C.; Kaçar, R. The effect of preheat & post weld heat treatment on the laser weldability of AISI 420 martensitic stainless steel. *Mater. Des.* **2014**, *64*, 221–226.
10. Köse, C. Weldability of 5754 aluminum alloy using a pulsed Nd:YAG micro scale laser. *Mater. Test* **2016**, *58*, 963–969. [[CrossRef](#)]

11. Köse, C. An investigation of the surface characterization of laser surface remelted and laser beam welded AISI 316L stainless steel. *Int. J. Electrochem. Sci.* **2016**, *11*, 3542–3554. [[CrossRef](#)]
12. Köse, C.; Kaçar, R. In vitro bioactivity and corrosion properties of laser beam welded medical grade AISI 316L stainless steel in simulated body fluid. *Int. J. Electrochem. Sci.* **2016**, *11*, 2762–2777. [[CrossRef](#)]
13. Li, C.; Li, B.; Wu, Z.; Qui, X.; Ye, B.; Wang, A. Stitch welding of Ti-6Al-4V titanium alloy by fiber laser. *Trans. Nonferr. Met. Soc. China* **2017**, *27*, 91–101. [[CrossRef](#)]
14. Caiazzo, F.; Cardaropoli, F.; Alfieri, V.; Sergi, V.; Argenio, P.; Barbieri, G. Disk-laser welding of Ti-6Al-4V titanium alloy plates in T-joint configuration. *Procedia Eng.* **2017**, *183*, 219–226. [[CrossRef](#)]
15. Chang, B.; Yuan, Z.; Pu, H.; Li, H.; Cheng, H.; Du, D.; Shan, J. A comparative study on the laser welding of Ti6Al4V alloy sheets in flat and horizontal positions. *Appl. Sci.* **2017**, *7*, 376. [[CrossRef](#)]
16. Taskin, M.; Caligulu, U.; Turkmen, M. X-ray tests of AISI 430 and 304 stainless steels and AISI 1010 low carbon steel welded by CO₂ laser beam welding. *Mater. Test.* **2011**, *53*, 741–747. [[CrossRef](#)]
17. Quintino, L.; Costa, A.; Miranda, R.; Yapp, D.; Kumar, V.; Kong, C.J. Welding with high power fiber lasers—A preliminary study. *Mater. Des.* **2007**, *28*, 1231–1237. [[CrossRef](#)]
18. Fu, P.; Mao, Z.; Zuo, C.; Wang, Y.; Wang, C. Microstructures and fatigue properties of electron beam welds with beam oscillation for heavy section TC4-DT alloy. *Chin. J. Aeronaut.* **2014**, *4*, 1015–1021. [[CrossRef](#)]
19. Casalino, G.; Mortello, M.; Campanelli, S.L. Ytterbium fiber laser welding of Ti6Al4V alloy. *J. Manuf. Process* **2015**, *20*, 250–256. [[CrossRef](#)]
20. Wang, S.H.; Wei, M.D.; Tsay, L.W. Tensile properties of LBW welds in Ti-6Al-4V alloy at evaluated temperatures below 450 °C. *Mater. Lett.* **2003**, *57*, 1815–1823. [[CrossRef](#)]
21. Ahmed, T.; Rack, H.J. Phase transformations during cooling in $\alpha+\beta$ titanium alloys. *Mater. Sci. Eng. A* **1998**, *243*, 206–211. [[CrossRef](#)]
22. Wang, S.; Wu, X. Investigation on the microstructure and mechanical properties of Ti-6Al-4V alloy joints with electron beam welding. *Mater. Des.* **2012**, *36*, 663–670. [[CrossRef](#)]
23. Kabir, A.S.H.; Cao, X.; Medraj, M.; Wanjara, P.; Cuddy, J.; Birur, A. Effect of welding speed and defocusing distance on the quality of laser welded Ti-6Al-4V. In Proceedings of the Materials Science and Technology (MS&T) Conference, Houston, TX, USA, 17–21 October 2010; pp. 2787–2797.
24. Sundaresan, S.; Ram, G.D.J.; Reddy, G.M. Microstructural refinement of weld fusion zones in a-b titanium alloys using pulsed current welding. *Mater. Sci. Eng. A* **1999**, *262*, 88–100. [[CrossRef](#)]
25. Li, X.; Xie, J.; Zhou, Y. Effects of oxygen contamination in the argon shielding gas in laser welding of commercially pure titanium thin sheet. *J. Mater. Sci.* **2005**, *40*, 3437–3443.
26. Barreda, J.L.; Santamaria, F.; Azpiroz, X.; Irisarri, A.M.; Varona, J.M. Electron beam welded high thickness Ti6Al4V plates using filler metal of similar and different composition to the base plate. *Vacuum* **2001**, *62*, 143–150. [[CrossRef](#)]
27. Yunk, W.K.C.; Ralph, B.; Lee, W.B.; Fenn, R. An investigation into welding parameters affecting the tensile properties of titanium welds. *J. Mater. Process. Technol.* **1997**, *63*, 759–764. [[CrossRef](#)]
28. Tsay, L.W.; Tsay, C.Y. The effect of microstructures on the fatigue crack growth in Ti-6Al-4V laser welds. *Int. J. Fatigue* **1997**, *19*, 713–720. [[CrossRef](#)]
29. Mehdi, B.; Badji, R.; Ji, V.; Allili, B.; Deschaux-Beaume, F.; Soulie, F. Microstructure and residual stresses in Ti-6Al-4V alloy pulsed and unpulsed TIG welds. *J. Mater. Process. Technol.* **2016**, *231*, 441–448. [[CrossRef](#)]
30. Kabir, A.S.H.; Cao, X.; Gholipour, J.; Wanjara, P.; Cuddy, J.; Birur, A.; Medraj, M. Effect of postweld heat treatment on microstructure, hardness, and tensile properties of laser-welded Ti-6Al-4V. *Metall. Mater. Trans. A* **2012**, *43*, 4171–4184. [[CrossRef](#)]
31. Caiazzo, F.; Curcio, F.; Daurelio, G.; Minutolo, F.M.C. Ti6Al4V sheets lap and butt joints carried out by CO₂ laser: Mechanical and morphological characterization. *J. Mater. Process. Technol.* **2004**, *149*, 546–552. [[CrossRef](#)]

